Vortex blob method and its application to vortex sheet motion

AUTHOR(S):

Sakajo, T.

CITATION:

Sakajo, T.. Vortex blob method and its application to vortex sheet motion. 数理解析研究所講究録 1995, 922: 99-123

ISSUE DATE:

1995-09

URL:

http://hdl.handle.net/2433/59755

数理解析研究所講究録
922巻 1995年 99-123

Vortex blob method and its application to vortex sheet motion.

T. Sakajo

Research Institute for Mathematical Sciences,
Kyoto University, Kyoto 606-01, Japan

1 Introduction

Vortex sheet is a surface in an incompressible fluid across which the tangential component of fluid velocity has a jump discontinuity. It is often used as a mathematical model for Kelvin-Helmholtz instability, where a thin vorticity layer becomes unstable and large vortex structures appear. Such a surface can be observed in many fluid flow, and so the study of the motion of vortex sheet plays an important role in the field of fluid dynamics, especially in the understanding of turbulent flow. Although various researches have been done so far, many questions still remain. The evolution equation of vortex sheet contains singular kernel, which make it difficult to solve the equation both numerically and analytically. Chorin's vortex blob method is one of the most successful methods for numerical study of vortex sheet motions. This method can be done by using desingularized kernel instead of singular kernel in the equation of vortex motion. The convergence of this method is showed by Caflisch and Lowengrub[5]. This convergence theorem, however, is obtained up to the critical time when the curvature of vortex sheet becomes infinity.

Krasny[8, 9] showed clearly how vortex sheets roll up after the critical time using this method and concluded that when reducing the regularization parameter, most of the numerical solutions have the roll-up structure which is independent of the regularization parameter. Also, Nitsche and Krasny[15] applied the method to an axisymmetric vortex-sheet model in order to simulate an real experiment in which vortex ring formation occurs. They compared the numerical results with experimental ones, and noted that their numerical solution is a good approximation of real fluid flow.

The purpose of the present paper is to add new examples which demonstrate use-fullness of vortex blob method. We will show the results of two examples;(a) a vortex sheet motion in the presence of a uniform shear flow,(b) interactions of two vortex sheets.

In section 2, we state how to apply vortex blob method to the evolution equation of vortex sheet motion with singular kernel and how to discritize it. And we also explain numerical technique,"Krasny's Fourier Filter", in order to observe the long time evolution of vortex sheets accurately. Numerical computations of one vortex sheet in the presence of a uniform shear flow appears in Section 3. We consider the interactions of two vortex sheets in Section 4.

2 Chorins's vortex blob method and Fourier Filter

A vortex sheet can be represented by the curve $\vec{R} \ni \Gamma \mapsto z(\Gamma, t) \in \vec{C}$ with Γ being taken along the curve. Γ is called the circulation parameter and t is time. We impose periodic boundary condition on vortex sheet,

$$z(\Gamma + 1, t) = z(\Gamma, t) + 1.$$

The motion of a vortex sheet with periodic boundary condition is known (Saffman[17]) to be governed by the following Birkhoff-Rott equation,

$$\frac{\partial z(t,\Gamma)^*}{\partial t} = \frac{1}{2i}\,\mathrm{p.v.}\int_0^1 \cot\pi\left(z(t,\Gamma) - z(t,\Gamma')\right) d\Gamma', \tag{1}$$

where the integral is Cauchy's principal value, $i = \sqrt{-1}$, and $*$ implies the complex conjugate. This equation is ill-posed (see Saffman[17]) and integration of the solutions breaks down unless certain devices are used. In vortex blob method, we desinguralize the equation (1) in such a way to replace the singular kernel to a regular kernel as below.

$$\frac{\partial z(t,\Gamma)^*}{\partial t} = \int_0^1 K_\delta(z(t,\Gamma) - z(t,\Gamma'))d\Gamma', \tag{2}$$

where the kernel function K_δ is defined as follows:

$$_K\delta(x+iy) = -\frac{1}{2}\frac{\sinh(2\pi y) + i\sin(2\pi x)}{\cosh(2\pi y) - \cos(2\pi x) + \delta^2}.$$

Note that the equation (2) reduces to (1) when $\delta = 0$. The equation is well-posed for any time interval if $\delta > 0$. The high frequency modes are stabilized.

We discretize (2) by the point vortices. Choosing a positive integer N, we consider the following system of ordinary differential equations:

$$\frac{\partial z_n(t)^*}{\partial t} = \sum_{1\leq m\leq 1, m\neq n} K_\delta(z_n(t) - z_m(t)), \tag{3}$$

When we get $\{z_n(t)\}_{1\leq n\leq N}$, which approximate the vortex sheet at time t, we integrate (9) to obtain $\{z_n(t+\Delta t)\}_{1\leq n\leq N}$. A fourth order Runge-Kutta method is used to integrate the ODEs. Then we let it go through the Fourier filter as Krasny did. Repeating this process, we can simulate the dynamics of the vortex sheet.

The desingularized equation (2) is well-posed, but in practical computation the round-off errors occur and deteriorate the computation eventually. In order to get a long time evolution of vortex sheet accurately, "Fourier Filtering" scheme introduced by R.Krasny[9] is effective. Assume that the solution of the equation (9) is given by the following form,

$$z(\Gamma, t) = \Gamma + \sum_{n=-\frac{N}{2}}^{\frac{N}{2}-1} a_n \exp 2\pi i n\Gamma$$

The second term is the disturbance from the steady solution ($z = \Gamma$) of the equation (9).

"Fourier Filtering" scheme can be done by the following steps.

1. Calculate $z_i(t) \rightarrow z_i(t + \Delta t)$ using forth order Runge-Kutta method.
2. Apply Fast Fourier Transformation algorithm to $z_i(t + \Delta t) - \frac{i}{N}$, and obtain coefficients of the disturbance term a_n.
3. For each coefficients a_n, if a_n doesn't exceed some threshold, we reset it to 0.(Filtering)
4. Get new $z_i(t + \Delta t)$ using Inverse Fourier Transformation with the filtered a_n.

Vortex blob method with Fourier Filter make it possible to get a long time vortex sheet calculation. For more detail, see [9].

3 A vortex sheet in a uniform shear

We now consider a vortex sheet in a uniform shear.

3.1 Equation and its linear analysis

Specifically, we consider the following equation:

$$\frac{\partial z(t,\Gamma)^*}{\partial t} = \frac{1}{2i}\,\mathrm{p.v.}\int_0^1 \cot\pi\,(z(t,\Gamma)-z(t,\Gamma'))\,d\Gamma' + G\mathrm{Im}z(t,\Gamma), \qquad (4)$$

A uniform shear term, $GIm[z(\Gamma,t)]$, is added to the Birkhoff-Rott equation (1). G is the constant representing the strength of the shear. When $G=0$, the equation is the same as Krasny used in [8, 9]. Note that we have neglected the influence of the vortex sheet on the background flow.

Because of the simplicity of (4), we can use vortex blob method stated in Section 2 without any change. But by a certain reason which we explain later, our equation with nonzero G requires a larger number of point vortices than are needed in the case of $G=0$. This makes our problem technically more difficult.

However, the phenomenological difference between the case of $G=0$ and that of $G\neq 0$ is far beyond the technical difference: we will show that this simple equation yields some interesting phenomena if we vary G. In fact, when $G>0$, we obtained some unexpected motions which the authors had not imagined from the case of $G=0$.

It well-known that the integral equation (4) with $G=0$ is ill-posed in the sense that a disturbance of wave number n is amplified by a factor proportional to $|n|$ (see Chapter 8 of Saffman [17], for instance). We study the stability of the stationary solution $z\equiv\Gamma$ in the case of nonzero G. This analysis was done by Kiya and Arie [7] based on the linearization of the Euler equations. We study the linearized equation of (4) and derive the same conclusion as theirs.

The linearization of (4) around $z\equiv\Gamma$ yields

$$\frac{\partial \zeta(t,\Gamma)^*}{\partial t} = -\frac{\pi}{2i}\,\mathrm{p.v.}\int_0^1 \frac{\zeta(t,\Gamma)-\zeta(t,\Gamma')}{\sin^2\pi(\Gamma-\Gamma')}d\Gamma' + G\mathrm{Im}\zeta(t,\Gamma), \qquad (5)$$

where use has been made of

$$\mathrm{p.v.}\int_0^1 \cot(\pi x)dx = 0.$$

We would like to analyze how unstable the zero solution $\zeta\equiv 0$ is. We now substitute

$$\zeta = \sum_{n=-\infty}^{+\infty} A_n(t)e^{2n\pi\Gamma i},$$

into (5) and take the $e^{2n\pi\Gamma i}$ mode only. We then obtain

$$\frac{dA_{-n}(t)^*}{dt} = \frac{\pi i}{2}\int_0^1 \frac{1-\cos(2n\pi x)}{\sin^2(\pi x)}dx A_n(t) + \frac{G}{2i}(A_n - A_{-n}^*)$$

for each $n = \pm 1, \pm 2, \cdots$. On the other hand, we have

$$\int_0^1 \frac{1-\cos(2n\pi x)}{\sin^2(\pi x)} dx = 2|n|$$

by the residue calculus. Therefore we obtain

$$\frac{dA_{-n}(t)^*}{dt} = \pi i|n|A_n(t) + \frac{G}{2i}(A_n - A_{-n}^*).$$

Replacing n with $-n$ and applying $*$ operator, we have

$$\frac{dA_n(t)}{dt} = -\pi i|n|A_{-n}(t)^* + \frac{G}{2i}(A_n - A_{-n}^*).$$

These two equations are written in the following form:

$$\frac{d}{dt}\begin{pmatrix} A_{-n}(t)^* \\ A_n(t) \end{pmatrix} = \begin{pmatrix} -\frac{G}{2i} & \frac{G}{2i} + \pi i|n| \\ \frac{G}{2i} - \pi i|n| & \frac{G}{2i} \end{pmatrix} \begin{pmatrix} A_{-n}(t)^* \\ A_n(t) \end{pmatrix}. \tag{6}$$

The characteristic polynomial of the matrix in the right hand side is

$$X^2 + \frac{G^2}{4} - \left| -i\frac{G}{2} + \pi i|n| \right|^2. \tag{7}$$

The eigenvalues are:

$$\pm\sqrt{\pi^2 n^2 - G\pi|n|}. \tag{8}$$

So, disturbances of mode n are neutrally stable if $G > \pi|n|$. This is exactly what was obtained by Kiya and Arie [7].

The result of this analysis may be summarized as follows:

- negative G enhances the instability of the flat vortex sheet;
- positive G neutralizes perturbation of low frequency.

The second observation led the authors to imagine that the instability occurs at a later time stage when $G > 0$. Also we thought that, if $G > \pi$, then the instability is realized as roll-ups with two or more "eye"s in the fundamental length $0 < \Gamma < 1$. We began our numerical experiments to examine this heuristic argument.

3.2 Discritization and numerical results

We discretize (2) by the point vortices. Choosing a positive integer N, we consider the following system of ordinary differential equations:

$$\frac{\partial z_n(t)^*}{\partial t} = \sum_{1 \le m \le 1, m \ne n} K_\delta(z_n(t) - z_m(t)) + G\mathrm{Im} z_n(t), \tag{9}$$

Parameters of discritization and desingularization are

- N, spatial discretization parameter(number of vortices),
- Δt, temporal step size,
- δ, desingularization parameter.

We computed vortex sheets when $G = -1.5\pi, 0, 0.5\pi, 1.5\pi, 2.5\pi$. In each run, the initial condition is

$$z(0,\Gamma) = \Gamma + 0.01(1-i)\sin 2\pi\Gamma,$$

namely

$$z_n(0) = \frac{n}{N} + 0.01(1-i)\sin\left(\frac{2\pi n}{N}\right), \qquad (n = 1, 2, \cdots, N)$$

which is the same as what Krasny chose. Parameters are chosen as follows: $\delta = 0.075, N = 512, \Delta t = 0.001$. As for the choice of δ and N, we tested other combinations; combinations of $\delta = 0.0375, 0.075, 1.0$ and $N = 256, 512, 1024$ were tested. We found that the above choice is most suited in the sense that numerical instability appears latest.

Figure 1 shows the time evolution when $G = 0$. Little visible difference is found between ours and Krasny's, showing our program's validity. However, the scales of the $x-$ and $y-$ axes are slightly different, which make our rolls look more oblate than Krasny's. But this is simply a matter of scaling, only. The same remark applies to the following figures, too. Figure 2 shows the case of $G = -1.5\pi$. This is similar to Figure 1, except that the roll is more oblate, which is intuitively obvious, and that the roll appears earlier. Figure 3 shows the evolution when $G = 0.5\pi$. The figure displays no qualitative difference from the previous cases except that the roll appears later, which agrees with the linear analysis.

We next consider the case where $G = 1.5\pi$. In this case, the magnitude of A_1 and A_{-1} do not increase in the valid range of the linearized equation. This suggests that the "one-eyed" roll-up observed by Krasny is unlikely to be seen in this case. In fact our computation shows that more than one roll-up appears in the fundamental wave length $0 < \Gamma < 1$. The coefficients A_1 and A_{-1} actually show no significant growth even in the nonlinear evolution, which is clearly seen in Figure 6. Figure 4 shows the time evolution of the vortex sheet. In the early stage ($1 < t < 1.6$), three vortex roll-ups are seen: Two of them are larger than the one near the center. Since the vortex sheet is symmetric about the origin, this suggests that two singularities occur first and another singularity occurs at the center soon after that. As time goes on, the rolls become larger and we see a "three-eyed" vortex sheet. At $t \approx 1.8$, another pair of singularities is created and we have a "five-eyed" vortex sheet afterwards. We computed up to $t \leq 3.0$ but the numerical instability was unavoidable when $t > 2.6$ and we do not know the monotone increase of

rolls manifests in the present situation. Anyway, this sounds curious since the positive G implies stabilization of the vortex sheet as far as the linear analysis can be applied. The naive stabilization is far from the truth. The temporal increase of the number of singularities makes a contrast to the case of $G = 0$. Krasny [10] shows the vortex roll-up for rather long time interval when $G = 0$. It shows quite a big deformation of the roll but shows no sign of the birth of new rolls.

The linear analysis suggests that the number of singularities may bigger when $G > 2\pi$. We computed when $G = 2.5\pi$ to obtain Figure 5. Seven eyes are observed at time $t = 2.6$ the first singularities appear near both ends of the interval. Figure 6 shows how the Fourier coefficients evolve with time.

3.3 Conclusion

The structure of singularities is qualitatively the same as that in the case of zero shear, when the shear works in the direction which strengthens the instability of the flat sheet. It is, however, quite different, when the shear works in the stable direction. Our computation seems to indicate that the number of singularities increases with time. Since the disturbance of low frequency is stabilized by the presence of a uniform shear, the time when first singularity emerges is delayed. As a result, however, the disturbance of high frequency have a effect on vortex sheet motion and many roll-up are observed.

4 Interactions of two vortex sheets

Two vortex sheet model has been studied in very many researches in order to simulate von Kármán-type flow which is a fluid flow through a bluff body. Krasny[11] observed that the wake in a streaming flow using vortex blob method for vortex-dipole sheet model numerically and compared with real experimental flow. Bögers [4] uses this method for two vortex sheet model, too. Other numerical method was applied to this type of flow; Vortex in Cell method (Aref and Siggia[1]) and point vortex approximation (Lin and Sirovich [12], Boldman, Brinch, and Goldstein [3]).

Our purpose is not to simulate von Kármán vortex streets, but to observe the mutual interactions between two sheets with various parameters, which are

- distance between two sheets,
- initial phase difference of two sheets,
- strength of two sheets.

4.1 Governing equations and its desingularization

The equation which describes the motion of two vortex sheet is a natural extension of the Birkhoff-Rott equation. We may add the contribution of other sheet to the Birkhoff-Rott equation itself. We define the complex-valued functions $z(\Gamma,t), w(\Gamma,t)$ as the representation of two vortex sheet's positions. (Γ is Lagrangian parameter, t is time.) Periodic boundary condition is imposed to both sheets,

$$\begin{aligned} z(\Gamma+1,t) &= z(\Gamma,t)+1 \\ w(\Gamma+1,t) &= w(\Gamma,t)+1 \end{aligned}$$

Then, we obtain the governing equations of two vortex sheets,

$$\begin{aligned} \frac{\partial z^*}{\partial t} &= \frac{\sigma_1}{2i} p.v. \int_0^1 \cot\pi(z(\Gamma,t)-z(\Gamma',t))d\Gamma' \\ &\quad + \frac{\sigma_2}{2i}\int_0^1 \cot\pi(z(\Gamma,t)-w(\Gamma',t))d\Gamma', \\ \frac{\partial w^*}{\partial t} &= \frac{\sigma_2}{2i} p.v. \int_0^1 \cot\pi(w(\Gamma,t)-w(\Gamma',t))d\Gamma' \\ &\quad + \frac{\sigma_1}{2i}\int_0^1 \cot\pi(w(\Gamma,t)-z(\Gamma',t))d\Gamma', \end{aligned} \tag{10}$$

where $*$ is complex conjugate operator, σ_1, σ_2 are the strength of two vortex sheets, respectively. $p.v.$ means the Cauchy principal value. Initial conditions of two sheets are given by the same one as Krasny's.

$$\begin{aligned} z(\Gamma,0) &= \Gamma + \epsilon\sin 2\pi\Gamma - i\epsilon\sin 2\pi\Gamma + \frac{iH}{2} \\ w(\Gamma,0) &= \Gamma + \epsilon\sin 2\pi\Gamma - i\epsilon\sin 2\pi(\Gamma+\alpha) - \frac{iH}{2} \end{aligned}$$

Here, H is the average distance between two sheet and α represents the phase difference between two sheets, respectively. ϵ is the amplitude of disturbance.

We apply Chorin's Vortex blob method as the numerical method. Using some non-negative parameter δ, we regularize the equation (10) as following.

$$\begin{aligned} \frac{\partial x_z}{\partial t} &= -\frac{\sigma_1}{2}\int_0^1 \frac{\sinh(y_z-y_z')}{\cosh 2\pi(y_z-y_z')-\cos 2\pi(x_z-x_z')+\delta^2} \\ &\quad -\frac{\sigma_2}{2}\int_0^1 \frac{\sinh(y_z-y_w')}{\cosh 2\pi(y_z-y_w')-\cos 2\pi(x_z-x_w')+\delta^2}, \\ \frac{\partial y_z}{\partial t} &= \frac{\sigma_1}{2}\int_0^1 \frac{\sin(x_z-x_z')}{\cosh 2\pi(y_z-y_z')-\cos 2\pi(x_z-x_z')+\delta^2} \\ &\quad +\frac{\sigma_2}{2}\int_0^1 \frac{\sin(x_z-x_w')}{\cosh 2\pi(y_z-y_w')-\cos 2\pi(x_z-x_w')+\delta^2}, \end{aligned} \tag{11}$$

$$\frac{\partial x_w}{\partial t} = -\frac{\sigma_2}{2}\int_0^1 \frac{\sinh(y_w - y_w')}{\cosh 2\pi(y_w - y_w') - \cos 2\pi(x_w - x_w') + \delta^2}$$
$$-\frac{\sigma_1}{2}\int_0^1 \frac{\sinh(y_w - y_z')}{\cosh 2\pi(y_w - y_z') - \cos 2\pi(x_w - x_z') + \delta^2},$$
$$\frac{\partial y_w}{\partial t} = \frac{\sigma_2}{2}\int_0^1 \frac{\sin(x_w - x_w')}{\cosh 2\pi(y_w - y_w') - \cos 2\pi(x_w - x_w') + \delta^2}$$
$$+\frac{\sigma_1}{2}\int_0^1 \frac{\sin(x_w - x_z')}{\cosh 2\pi(y_w - y_z') - \cos 2\pi(x_w - x_z') + \delta^2},$$

where $z(\Gamma, t) = x_z(\Gamma, t) + iy_z(\Gamma, t)$ and $w(\Gamma, t) = x_w(\Gamma, t) + iy_w(\Gamma, t)$.

4.2 Numerical results

In what follows, only two types of the strength of two sheets are studied; (1) $\sigma_1 = 1, \sigma_2 = 1$, (2) $\sigma_1 = 1, \sigma_2 = -1$. We pay attention to their mutual interactions between two sheets. We investigate these characteristics with varying parameters. Numerical parameters N, Δt, and δ are chosen to be 2048, 0.01, and 0.1, respectively.

4.2.1 The case $(\sigma_1, \sigma_2) = (1, 1)$

Figure 7 shows the time evolution of two sheets with initial conditions $H = 0.1$ and $\alpha = 0$. At nearly $t = 0.6$, one roll-up emerges on each sheet simultaneously. These roll-ups are getting closer as time goes. At $t = 0.8$ new pair of roll-up appears. Consequently, at $t = 1.0$ two pairs of roll-ups construct a core region. On the other hand, the distance between trailing arms which connect with the core becomes thinner. Compared with the evolution of vortex layers[2], we can find that the structure of core regions are quite different. The core region constructed through two sheets motion has more complicated structure than vortex layer's. Does this core region structure changes if the desingularized parameter of vortex blob method $\delta \to 0$? In Figure 8, the core regions with $\delta = 0.05, 0.0625, 0.075, 0.0875, 0.1, 0.1125, 0.125, 0.1375$ at $t = 1.0$ are given. Except for winding number of roll-ups, the qualitative structure of core regions looks the same.

We consider the effect of initial distance H between two vortex sheets. Figure 9 is the time evolution of two vortex sheets with initial distance $H = 0.4$,$\alpha = 0$ in the right column and $H = 0.08$,$\alpha = 0$ in the left column. When $H = 0.4$, only one pair of roll-up appears and no core structure like $H = 0.1$ can be seen up to $t = 1.4$. Upper vortex sheet flows toward left and lower one goes to right, which seem to move independently of each other. When $H = 0.08$, the same vortical core structure appears as $H = 0.1$. However, the size of core region is smaller and the distance of trailing arm is thinner. We can conclude that the vortical core structure appears because of closer initial distance between sheets.

Our numerical results obtained above are executed with no initial phase difference, i.e. $\alpha = 0$. In this case, complicated vortical core structure can be found. It is natural to ask how does this core structure changes if we vary the initial phase difference. Figure 10 includes the vortical core structures formed through the motion of two vortex sheets with various initial phase differences; $\alpha = 0, 0.125, 0.25, 0.375, 0.5, 0.625, 0.75, 0.875$. In all cases, initial distance between two vortex sheets is fixed to $H = 0.1$. The positions and numbers of roll-ups are different. These vortical structures for various initial phase differences seem to change continuously with respect to α.

4.2.2 The case $(\sigma_1, \sigma_2) = (1, -1)$

This flow model corresponds to a flow through a bluff body. Many researches has been studied this flow [1, 3, 4, 10, 12]. In the same way as used in subsection 3.1, we consider the center position of spiral and the critical time of two vortex sheets with various combinations of initial conditions.

Although our purpose is not to observe von Kármń vortex streets, it is natural to begin our computation with the case that two vortex sheet are located to be symmetrical with respect to x-axis. Figure 11 shows the time evolution of two vortex sheets with initial condition $H = 0.1$ and $\alpha = 0.5$. This symmetry between two vortex sheets is conserved through the evolution, which is obvious from the governing equation. Both upper and lower sheets move towards right and at $t = 0.5$ one roll-up on each vortex sheet emerge. We can see a clockwise spiral on upper sheet and counterclockwise spiral on lower sheet. This motion of two vortex sheets reminds us of a jet flow.

Figure 12 shows the evolution of two vortex sheets with initial difference $\alpha = 0.5$. The right column in the Figure shows the numerical solution with $H = 0.4$ and the left column is the solution with $H = 0.1$. We can find that the evolution doesn't change qualitatively despite the change of H, which is different from the case $(\sigma_1, \sigma_2) = (1, 1)$.

Figure 13 are the numerical solutions at time $t = 1.0$ with various initial phase difference α. The initial distance of each computation is fixed to $H = 0.2$. When $\alpha = 0$, the position of upper vortex sheet spiral is located at the left-hand side of the position of lower spiral. As α increase, the position of upper spiral chase the positions of lower spiral. At $\alpha = 0.5$ the upper one catch up with the lower one and after pass it. However, at $\alpha = 0.875$ the upper one is at the left-side of the lower one again.

5 discussion

Chorin's vortex blob method with Krasny's Fourier Filter is quite useful to simulate vortex sheet motions. Vortex methods for vortex sheets are proved to converge in the Time range before any singularity appears ([5]). However,

the behavior of the vortex sheet after any singularity is not completely understood. It might be that no legitimate solution is available after singularity, let alone the validity of the Birkhoff equation (1). The authors learned this view by ([6]), in which Caflisch suggested the necessity to add the vanishing viscosity, in order to get a unique solution. He argues that if the singularity is a branch point, then only viscosity enables us to choose a unique solution. We, however, obtained no numerical indication of convergence to more than one solution after the singularity. Since we tested only one regularization, it will be too bold to say, but we think that it might be possible to obtain a unique solution after the singularity even in the category of inviscid fluid flow. Also, Tryggvason et al. [18] shows that a certain inviscid limit of viscous flow simulation converges to a roll which is very close to Krasny's roll. This seems to be an indirect evidence to support the uniqueness of convergence even after the emergence of singularity. We also comment that the resolution of branch point by a viscosity might not always be possible. Masuda's surprising theorem ([14]) on a certain semi-linear diffusion equation can be interpreted as such. His theorem says that a certain one-dimensional semi-linear diffusion equation has a unique solution past a blow-up time only if the solution is independent of the space variable, namely, only if the solution is trivial.

References

[1] H. Aref and E. Siggia, Evolution and breakdown of a vortex sheet in two dimensions, J. Fluid Mech. vol. 109 (1981), pp. 435-463.

[2] G.R. Shelley and M.J. Shelley, On the connection between thin vortex layers and vortex sheets, J. Fluid Mech. vol. 215 (1990), pp.161–194.

[3] D.R. Boldman, P.F. Brinich and M.E. Goldstein, Vortex shedding from a blunt trailing edge with equal and unequal external mean velocities, J. Fluid Mech. vol. 109 (1981) pp. 435–463.

[4] C. Bögers, On the numerical solution of the regularized Birkhoff equation, Math. Comp. vol. 53 (1989), pp. 141–156.

[5] R.E. Caflisch and J.S. Lowengrub, Convergence of the vortex method for vortex sheets, SIAM J. Numer. Anal., vol. 26 (1989), pp. 1060–1080.

[6] R.E. Caflisch, Analysis for the evolution of vortex sheets, Vortex Dynamics and Vortex Method, C.R. Anderson and C. Greengard eds. Amer. Math. Soc., (1991), pp. 67–83.

[7] M. Kiya and M. Arie, Helmholtz instability of a vortex sheet in uniform shear flow, Phys. Fluid, vol. 22 (1979), pp. 378–379.

[8] R. Krasny, A study of singularity formation in a vortex sheet by the point-vortex approximation, J. Fluid Mech., vol. 167 (1986), pp. 65–93.

[9] R. Krasny, Desingularization of periodic vortex sheet roll-up , J. Comp. Phys., vol. 65 (1986), pp. 292–313.

[10] R. Krasny, Computation of vortex sheet roll-up, Springer Lecture Notes in Math., # 1360 (1988), Eds., C. Anderson and C. Greengard, pp. 9–22.

[11] R. Krasny, Vortex Dynamics and Vortex Methods , Lectures in Applied Mathematics (1991), vol. 28 , pp. 385–402.

[12] C. Lin and L. Sirovich, Nonlinear vortex trail dynamics , Phys. Fluids vol. 31 (1988).

[13] D.W. Moore, The spontaneous appearance of a singularity in the shape of an evolving vortex sheet, Proc. R. Soc. Lond. A, vol. 365 (1979), pp. 105–119.

[14] K. Masuda, Blow-up of solutions of some nonlinear diffusion equations, in " Nonlinear PDE in Appl. Sci.", H. Fujita, P.D. Lax, and G. Strang , eds., North-Holland, (1983), pp. 119–131.

[15] M. Nitsche and R. Krasny, A numerical study of vortex ring formation at the edge of a cicular tube, J.Fluid Mech. (1994), vol. 276, pp. 139–161.

[16] C. Pozrikidis and J.J.L. Hidgon, Instability of compound vortex layers and wakes, Phys. Fluids vol. 30 (1987), pp. 2965–.

[17] P.G. Saffman, Vortex Dynamics, Cambridge Univ. Press, (1992).

[18] G. Tryggvason, W.J.A. Dahm, and K. Sbeih, Fine structure of vortex sheet rollup by viscous and inviscid simulation, J. Fluids Engineering, vol. 113 (1991), pp. 31–36.

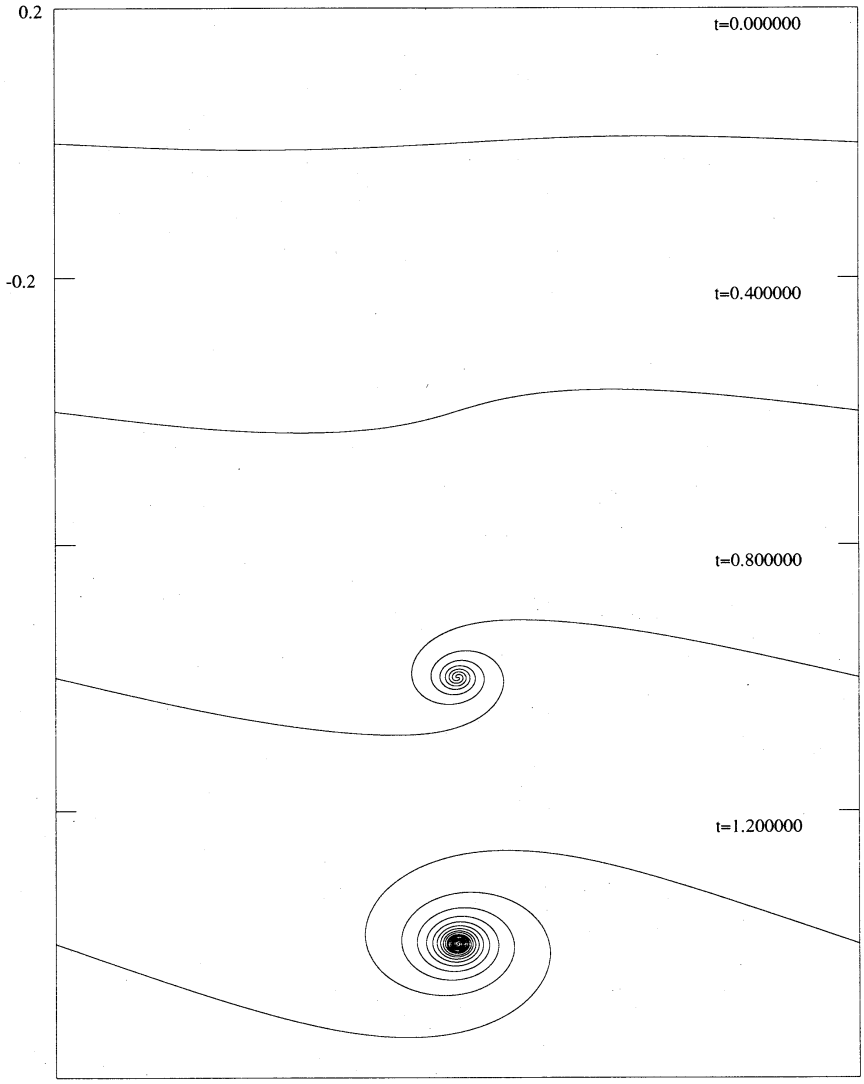

Figure 1: Time evolution of the vortex sheet. $G = 0$. Krasny's result is reproduced accurately. The scales of the $x-$ and $y-$ axes are slightly different, which make our rolls look more oblate than Krasny's. But this is simply a matter of scaling, only.

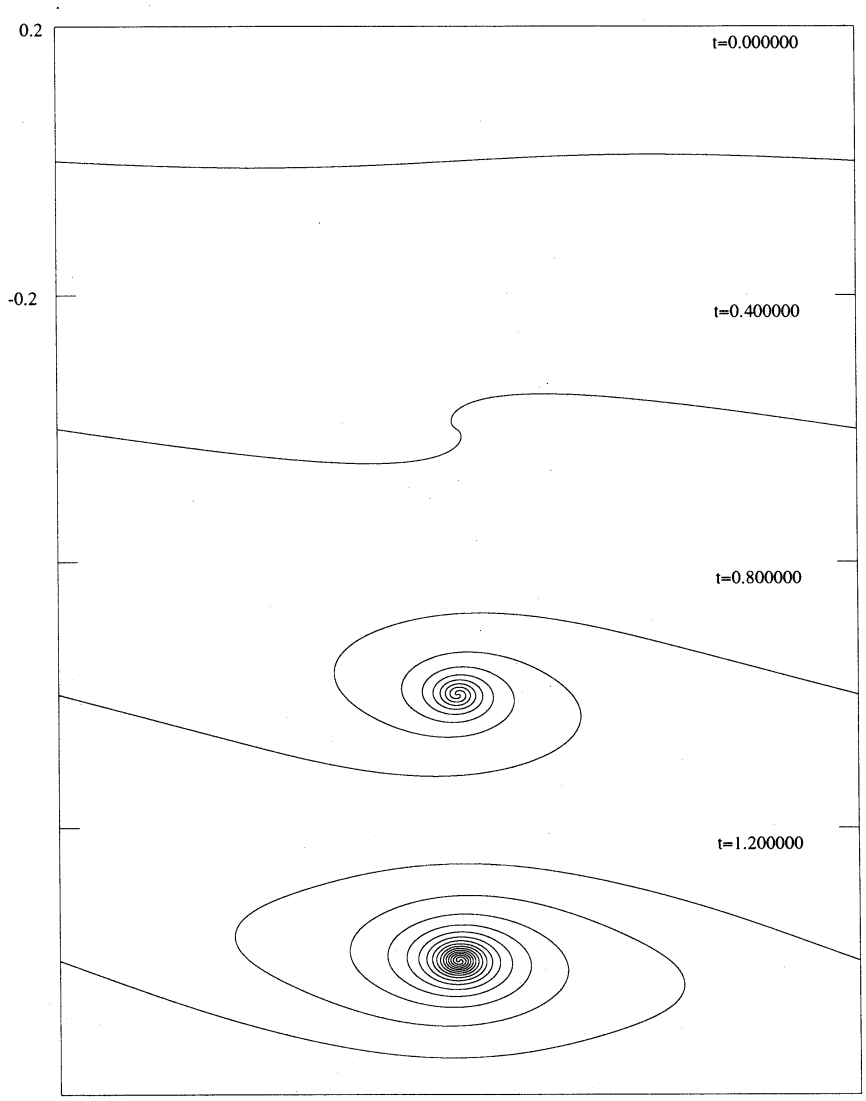

Figure 2: Time evolution of the vortex sheet. $G = -1.5\pi$. Qualitatively the same as Figure 1 but the roll-up appears earlier and the roll size is more oblate.

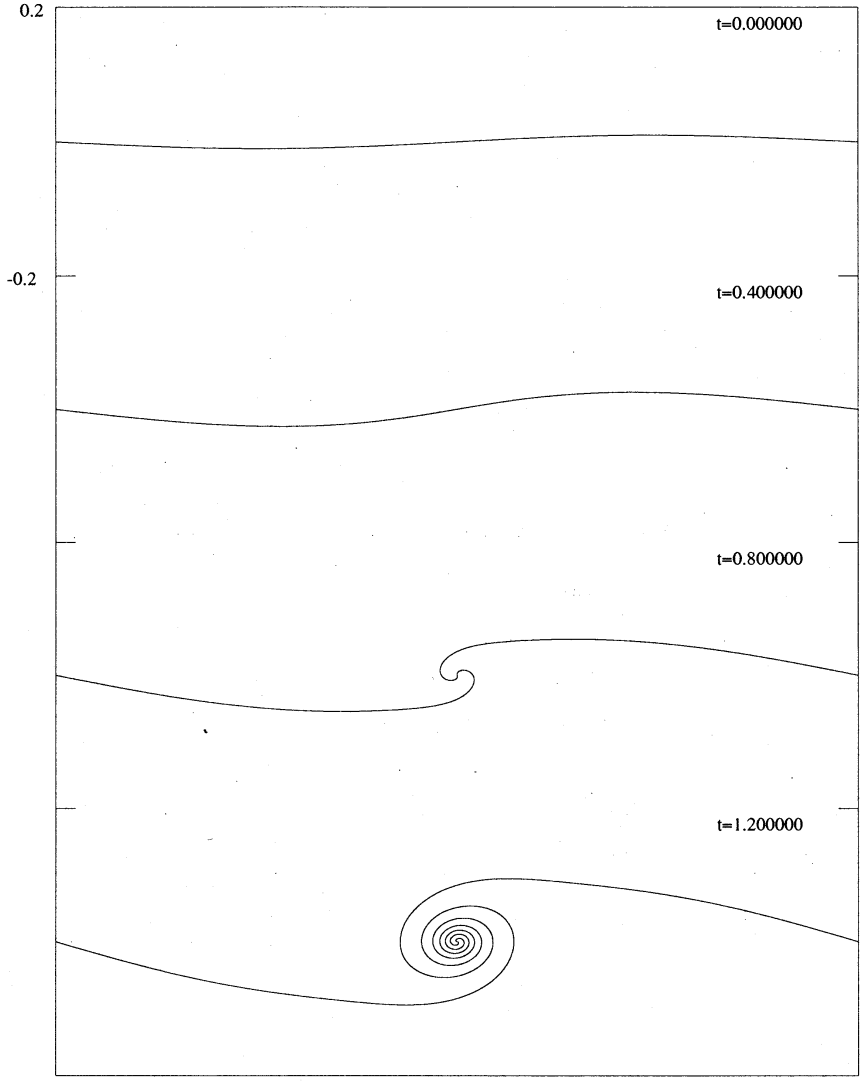

Figure 3: Time evolution of the vortex sheet. $G = 0.5\pi$.

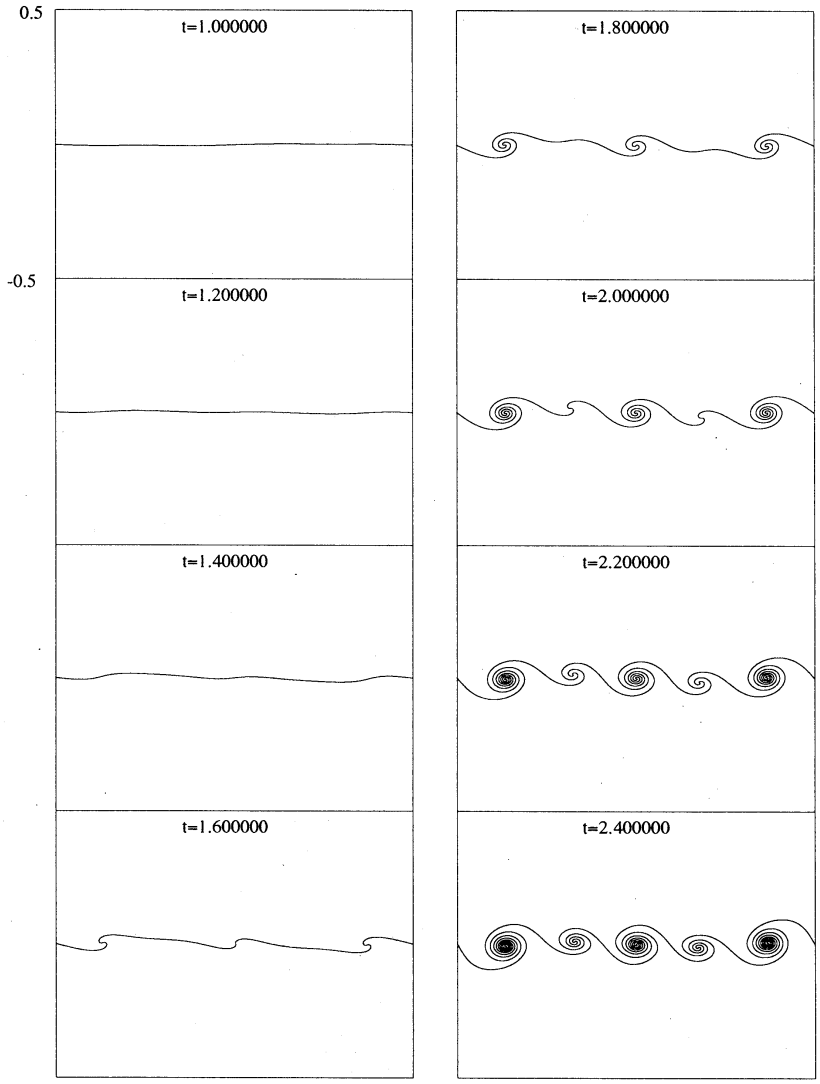

Figure 4: Time evolution of the vortex sheet. $G = 1.5\pi$. Singularities grow in number from one to five.

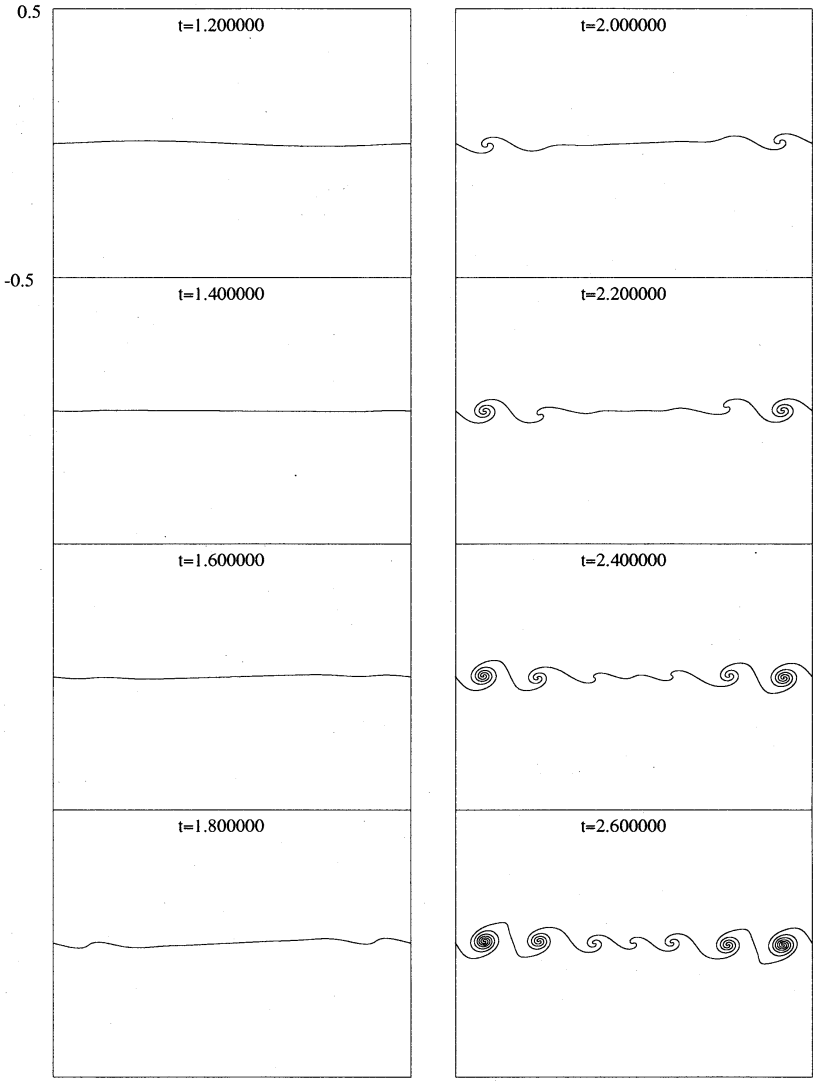

Figure 5: Time evolution of the vortex sheet. $G = 2.5\pi$.

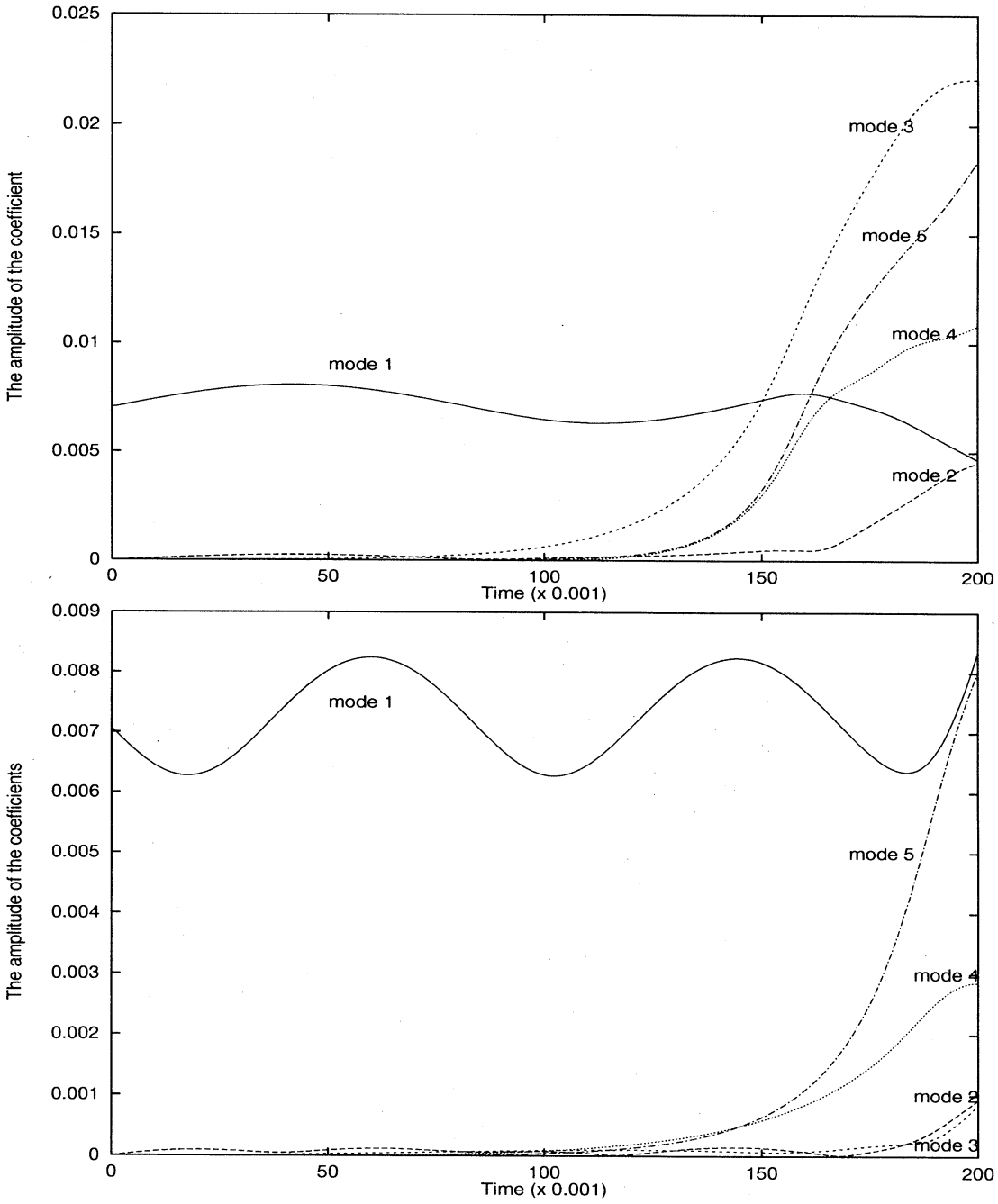

Figure 6: Time evolution of the Fourier coefficients $a_n = 1 \cdots$. $G = 1.5\pi$ (Upper),$G = 2.5\pi$(Lower).

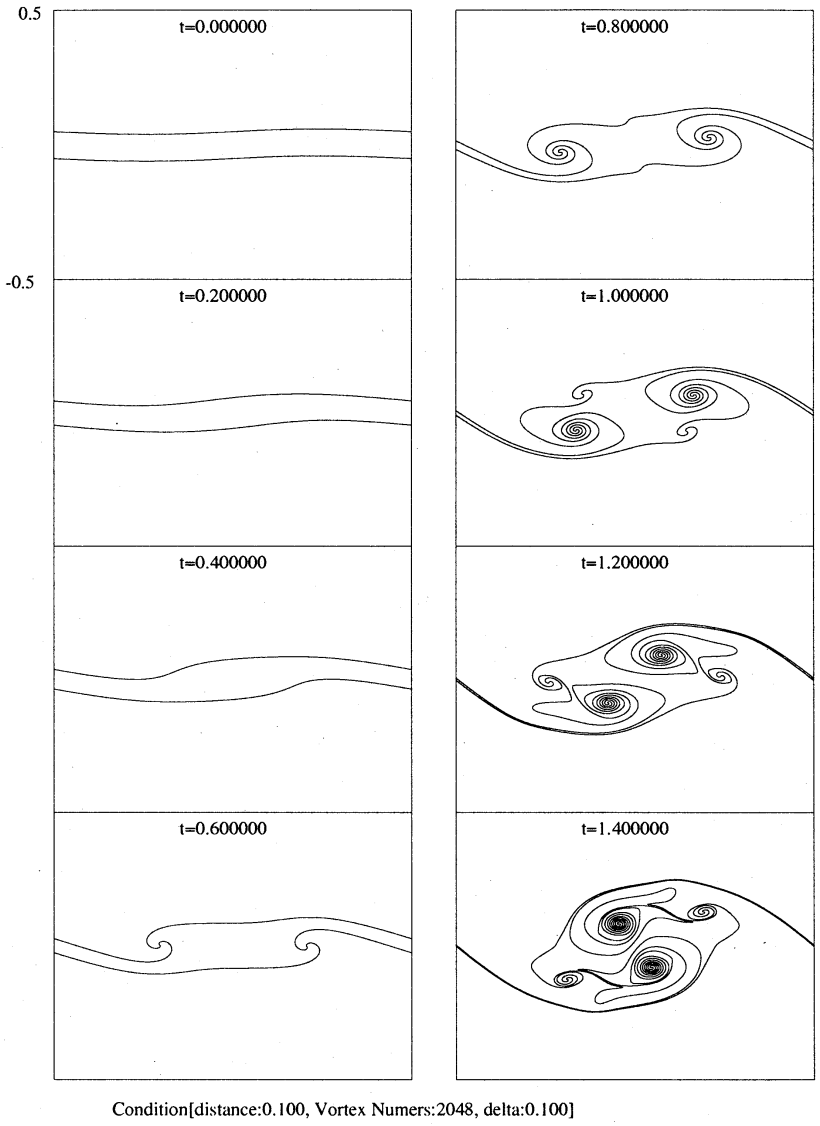

Figure 7: The time evolution of two vortex sheets with the same vorticity. The initial distance between sheets $H = 0.1$, initial phase difference $\alpha = 0$.

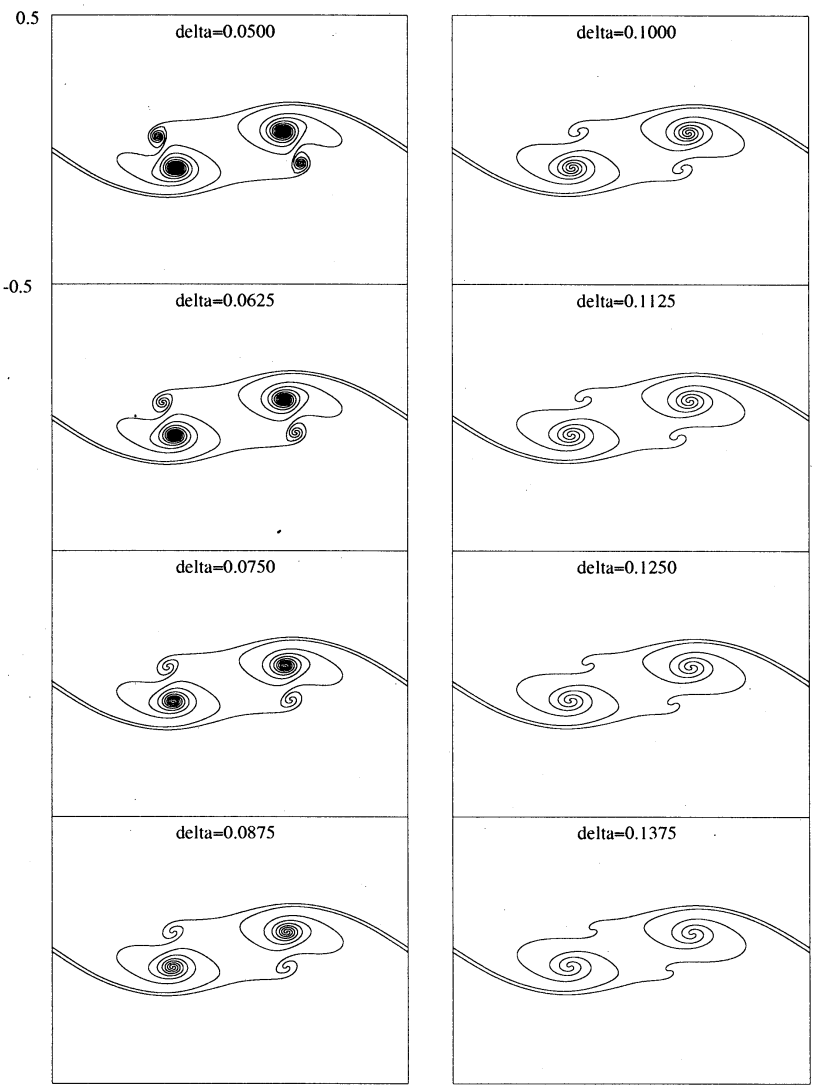

Figure 8: The core region of vortex sheet with various δ. The core structure looks universal except for rotating number of roll-ups.

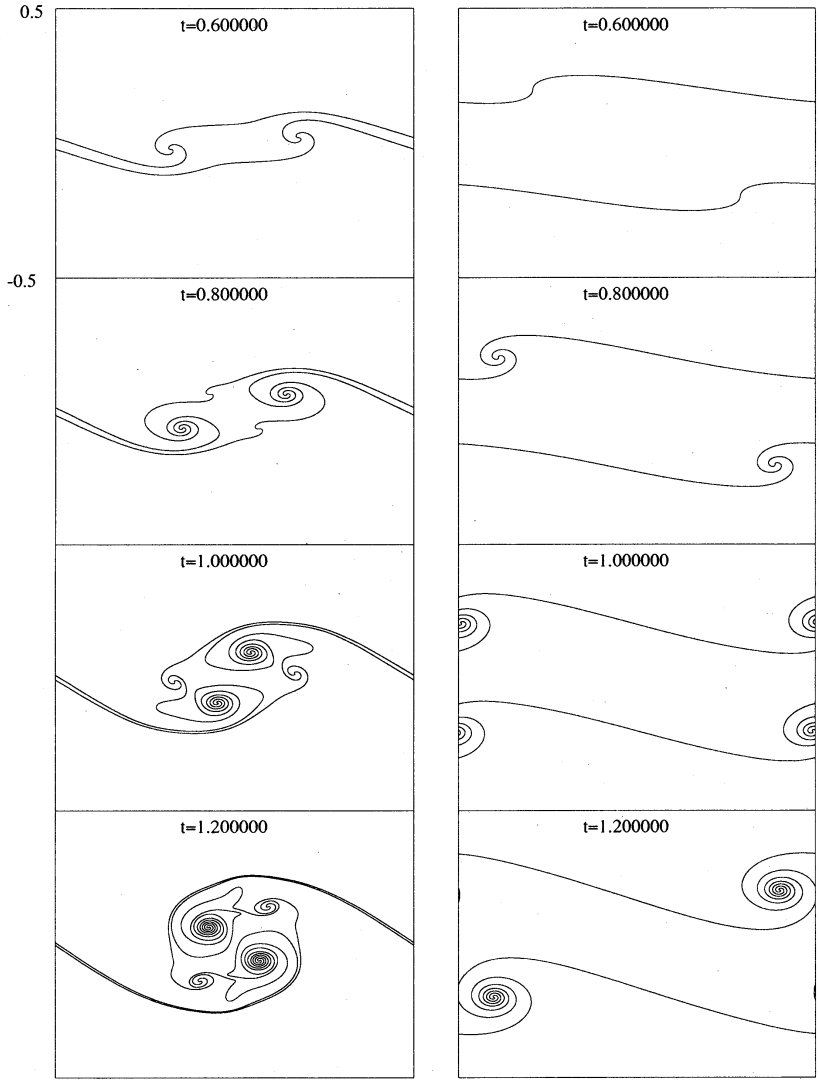

Figure 9: The time evolution of two vortex sheets with the same vorticity. The initial distance between sheets $H = 0.4$ in the right column, and $H = 0.08$ in the left column. Their initial phase difference are $\alpha = 0$.

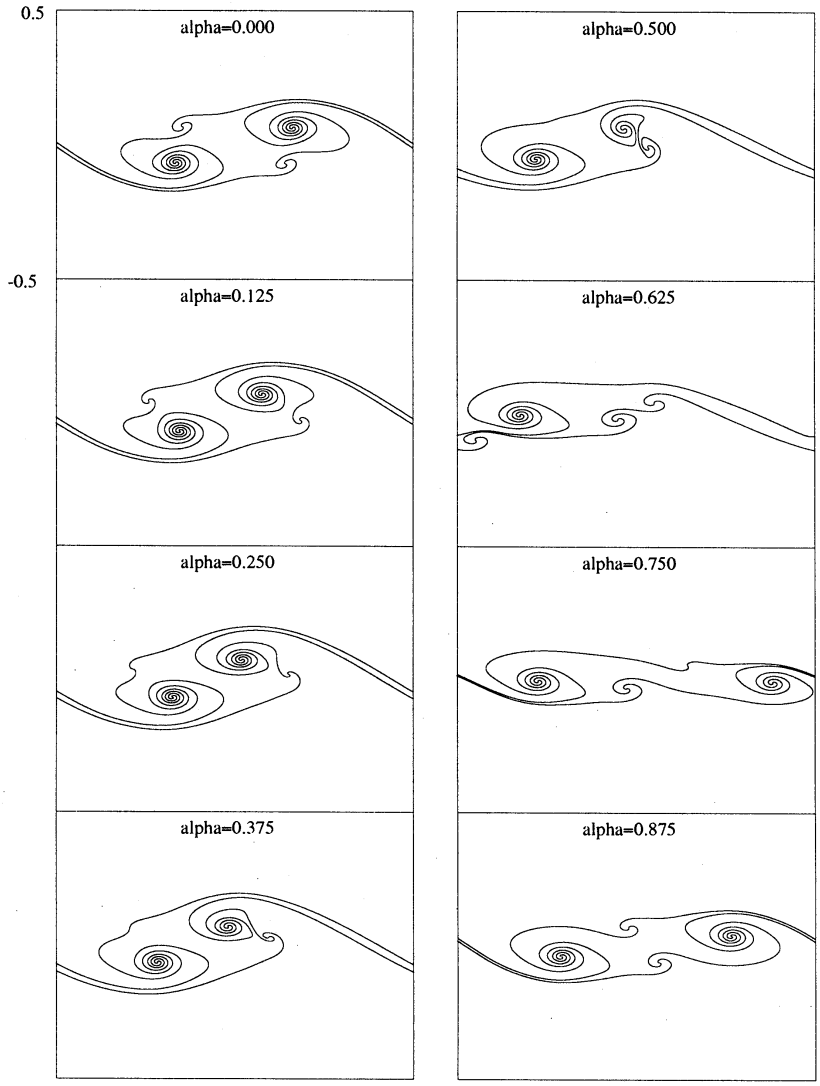

Figure 10: The numerical evolution of two vortex sheet in condition with various α at time $t = 1.0$. The initial phase difference is fixed to $H = 0.1$.

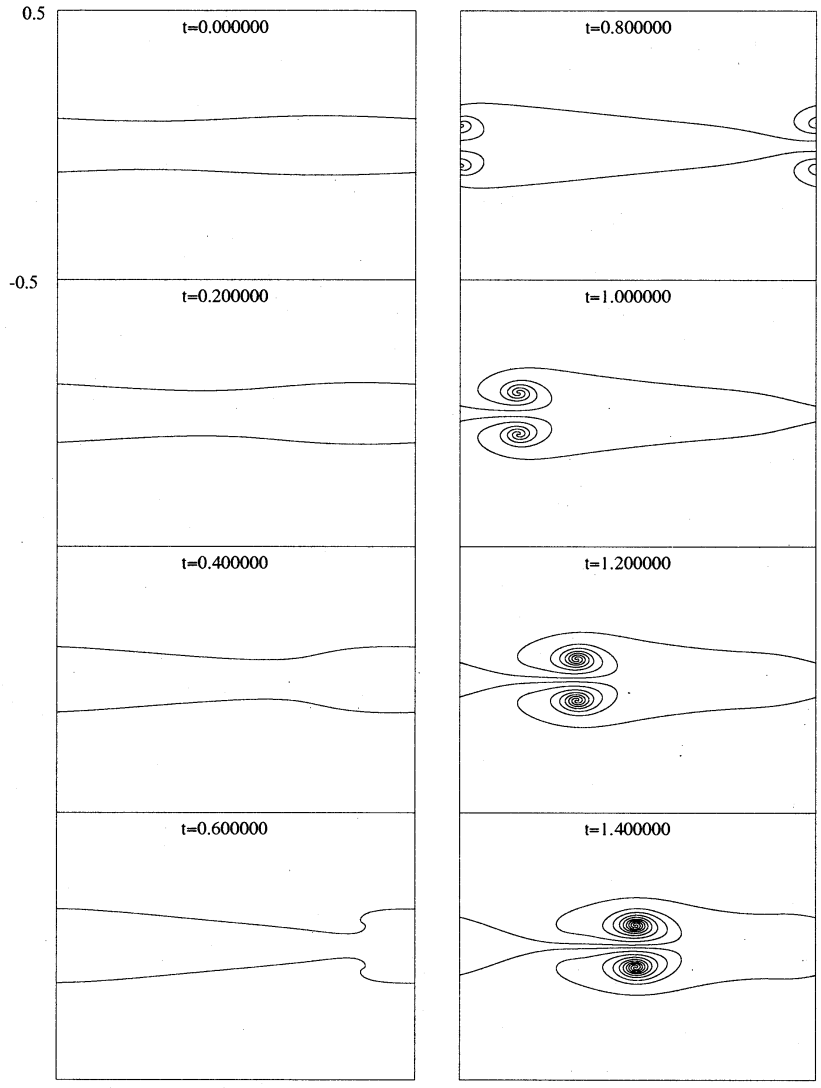

Figure 11: The evolution of two vortex sheets. Initial conditions of two vortex sheets are $\sigma_1 = 1, \sigma_2 = -1, H = 0.2$, and $\alpha = 0.5$(symmetric with respect to x-axis).

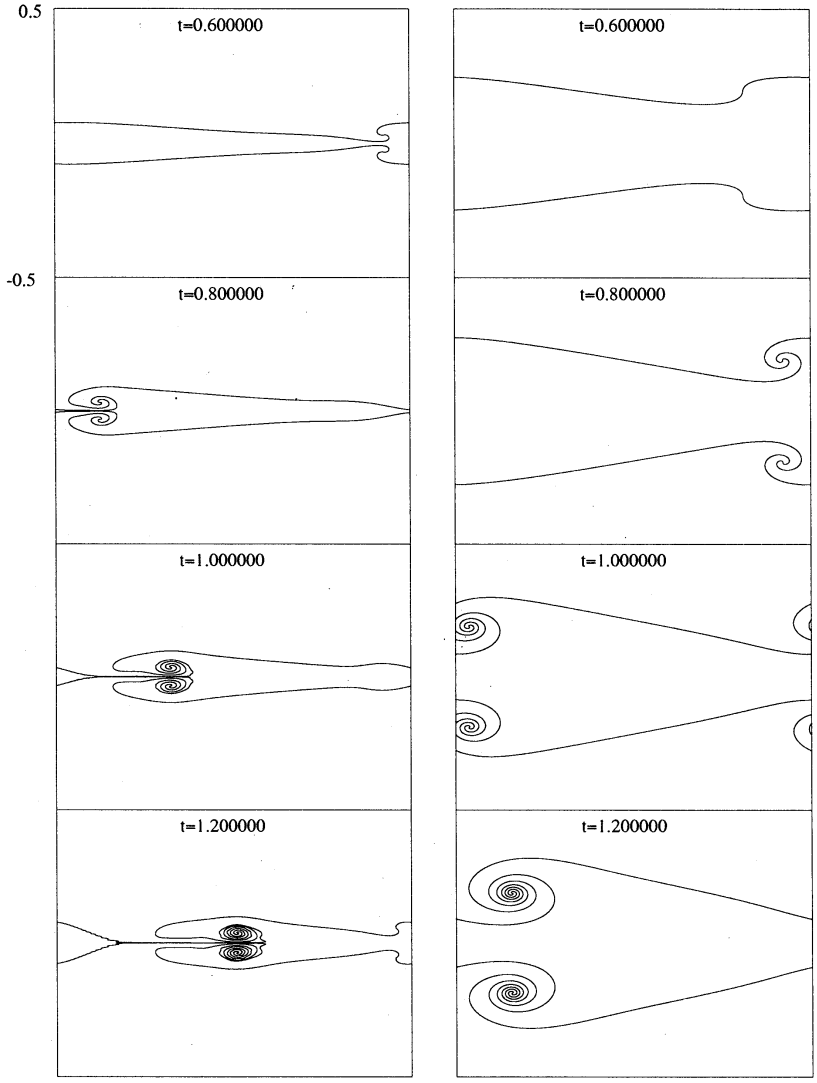

Figure 12: The evolutions of two sheets. The right column is the numerical solution $H = 0.4$, the left is with $H = 0.1$.

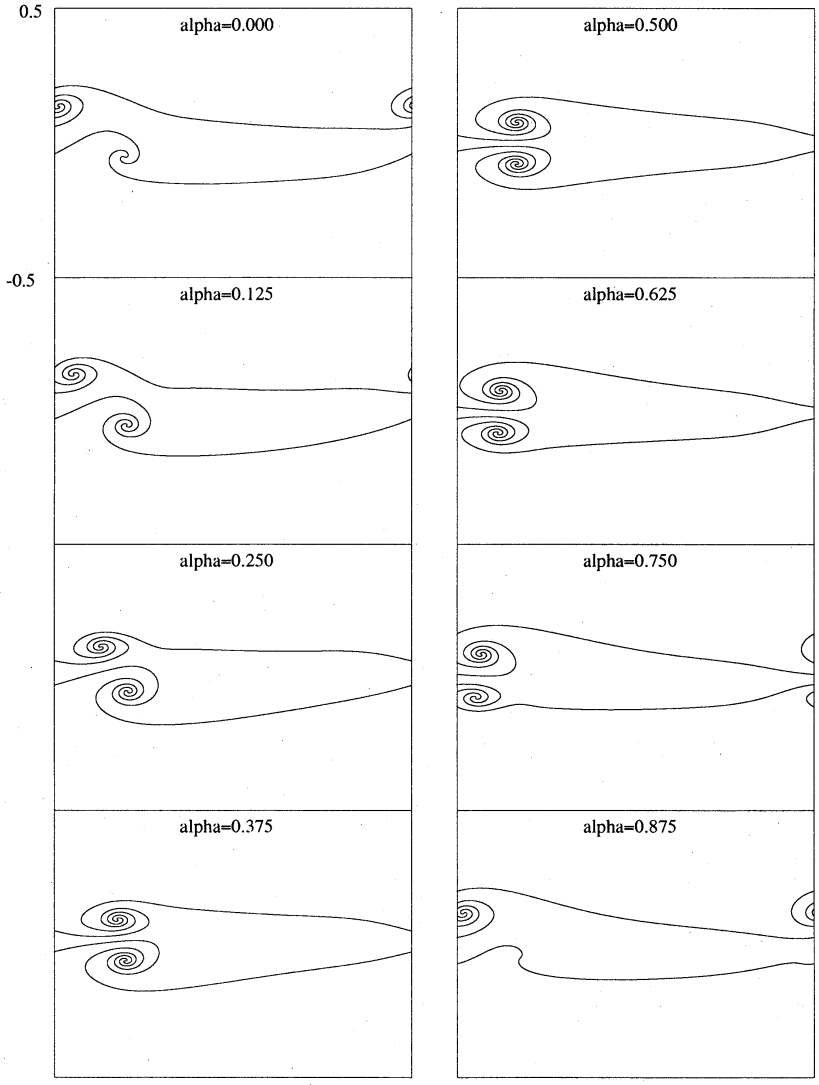

Figure 13: The numerical solutions of two sheet with the various initial phase differences $\alpha = 0.0, 0.125, 0.25, 0.375, 0.5, 0.625, 0.75, 0.875$. The initial difference between them are fixed to $H = 0.2$.